



Article

Modelling Yeast Prion Dynamics: A Fractional Order Approach with Predictor–Corrector Algorithm

Daasara Keshavamurthy Archana ¹, Doddabhadrappla Gowda Prakasha ^{1,*} and Nasser Bin Turki ²

¹ Department of Mathematics, Davangere University, Shivangotri, Davangere 577007, India; dkarchanamath01@gmail.com

² Department of Mathematics, College of Science, King Saud University, P.O. Box 2455, Riyadh 11451, Saudi Arabia; nassert@ksu.edu.sa

* Correspondence: prakashadg@gmail.com or prakashadg@davangereuniversity.ac.in

Abstract: This work aims to comprehend the dynamics of neurodegenerative disease using a mathematical model of fractional-order yeast prions. In the context of the Caputo fractional derivative, we here study and examine the solution of this model using the Predictor–Corrector approach. An analysis has been conducted on the existence and uniqueness of the selected model. Also, we examined the model's stability and the existence of equilibrium points. With the purpose of analyzing the dynamics of the Sup35 monomer and Sup35 prion population, we displayed the graphs to show the obtained solutions over time. Graphical simulations show that the behaviour of the populations can change based on fractional orders and threshold parameter values. This work may present a good example of how biological theories and data can be better understood via mathematical modelling.

Keywords: Caputo fractional derivative; neurodegenerative disease; yeast prion model; predictor–corrector method



Citation: Archana, D.K.; Prakasha, D.G.; Bin Turki, N. Modelling Yeast Prion Dynamics: A Fractional Order Approach with Predictor–Corrector Algorithm. *Fractal Fract.* **2024**, *8*, 542. <https://doi.org/10.3390/fractalfract8090542>

Academic Editor: Bruno Carpentieri

Received: 1 August 2024

Revised: 3 September 2024

Accepted: 17 September 2024

Published: 19 September 2024



Copyright: © 2024 by the authors. Licensee MDPI, Basel, Switzerland. This article is an open access article distributed under the terms and conditions of the Creative Commons Attribution (CC BY) license (<https://creativecommons.org/licenses/by/4.0/>).

1. Introduction

We will refer to derivatives and integrals with any order as fractional calculus (FC). Leibnitz created non-integer derivatives after creating integer order derivatives. The mathematical basis of arbitrary order derivatives was developed in collaboration with numerous researchers [1–5]. It has been found that FC offers a systematic and efficient exposition of the reality of nature and that it is more beneficial than classical calculus for modelling real-world difficulties. When developing methods to simulate models, fractional differential equations (FDEs) are becoming more and more significant. Whichever order, the solutions to these FDEs are essential for describing the characteristics and nature of complicated issues that arise in applied mathematics and technology. It is extremely difficult to find solutions for these DEs, nevertheless. One of the most helpful and effective methods in applied mathematics for resolving this problem has been the development of integral transformations, which have found wide-ranging applications in disciplines like biology [6], financial market [7], complex fluids [8], human disease [9], nanotechnology [10], biotechnology [11], control vectors [12], fluid dynamics [13], and many more [14–18].

Prions are proteins that have been most frequently connected to severe neurodegenerative diseases in humans, but they can also cause a variety of innocuous heritable phenotypes in yeast, and these several states occur when a protein emerges in an improperly folded state [19]. Recently, prion characteristics for several proteins implicated in amyloid and neuronal inclusion diseases were discovered. The occurrence of protein aggregation and amyloid formation has led to a rise in research activity across various scientific fields. The correlation between amyloid deposition and a number of severe diseases such as type II diabetes, Parkinson's disease, and Alzheimer's disease. In yeast, amyloids can proliferate steadily as prions, which are heritable units. In addition to being interesting on their own, yeast prions can be used as a model for amyloids and prions in general. It is possible for a

single instance of prion production to kill out a single person, a population within a species, or perhaps the entire species. Strong selection pressure is thus created for the cells that have defences against prions [20–24]. When guanidine hydrochloride is introduced to a proliferating culture of yeast cells containing some Sup35p protein in its prion form, the percentage of cells that contain prion-replicating units, or propagons, gradually declines over time [25,26]. In particular, when considering neurological diseases, modelling yeast prion dynamics is a crucial phase in understanding the biological population domain. Studies of disorders such as human Creutzfeldt–Jakob disease depend significantly on prions, which are misfolded proteins that can cause other proteins to misfold as well. Models for similar dynamics can be found in yeast, where prions like [PSI+] exist. Because they take into account both the population dynamics of the cells and the dynamics of the proteins within individual cells, the structured population models created for yeast prions are especially insightful. The field of neurodegenerative diseases is a major challenge faced by public health and is still in need of robust preventive measures and disease-modifying treatments. Biological population-based studies can offer the framework in the context of primary and secondary prevention of neurodegenerative diseases. The designed study will take into consideration the biological and phenotypical subtypes of disease also. Although key components of protein deposits or established genetic processes are used to classify neurodegenerative illnesses, current research has shown both intraindividual variations and overlap across various symptoms. Common pathogenic pathways may be suggested by synergistic mechanisms among diseased proteins. Further research and animal models have shed light on the fundamental processes behind neurodegeneration and cell death, opening up new avenues for preventative and therapeutic approaches in the future. The study of yeast prion dynamics via a fractional order approach offers a novel perspective in understanding neurodegenerative diseases. The use of fractional derivatives in mathematical modelling provides a more nuanced representation of biological systems, potentially leading to breakthroughs in how we understand and treat disorders like Alzheimer’s and Parkinson’s. So, in the context of fractional calculus, it will be more beneficial for addressing the dynamics of disease control.

In this work, we considered the yeast prion model which is a simple model as a system of two ordinary differential equations. So, we proposed a fractional-order form for this model to understand the dynamics of neurodegenerative disease. Predictor–Corrector (PC) technique has not yet been applied to address the proposed framework. Therefore, we employed the PC approach using the Caputo-type fractional derivative. These days [27–30], a number of studies have demonstrated that the suggested approach is successfully and extensively used in a variety of models because the considered technique is free from assumptions, discretization, large simplification and others. The PC approach has a few constraints. Errors can spread during the successive rounds of correction if the initial prediction is incorrect, particularly in long-term simulations. The step size selection has a significant impact on the method’s stability and accuracy. But this method frequently produces more accurate findings than other methods since it combines the prediction and correction phases into one step. When the solution to a problem evolves smoothly over time, the corrective step frequently produces superior convergence qualities than single-step techniques.

The current work is structured as follows: An introduction is given in Section 1. Section 2 provides the fundamental definitions. The considered model’s formulation and description are covered in detail in Section 3. The existence and uniqueness of the model are covered in Section 4. The stability of the model is shown in Section 5. Section 6 presents the PC approach solution for the model. Section 7 is a discussion part that includes the assembled graphical results and their implications. The conclusion is found in Section 8.

2. Preliminaries

Here, we review a few fundamental notions related to fractional derivatives and Mittag–Leffler function.

Definition 1. For a function $f(t) \in C_{-1}^n$, the fractional integral of order $\kappa \geq 0$ in terms of Riemann-Liouville [1] is specified as

$$I^\kappa f(t) = \frac{1}{\Gamma(\kappa)} \int_0^t (t-\tau)^{\kappa-1} f^{(n)}(\tau) d\tau, \kappa > 0, t > 0, \quad (1)$$

$$I^0 f(t) = f(t).$$

Here, $\Gamma(\cdot)$ represents the Gamma function.

Definition 2. The fractional derivative for a function $f \in C_{-1}^n$ is defined as follows in terms of Caputo [1]:

$$D_t^\kappa f(t) = \begin{cases} \frac{d^n f(t)}{dt^n}, & \kappa = n \in \mathbb{N}, \\ \frac{1}{\Gamma(n-\kappa)} \int_0^t (t-\tau)^{n-\kappa-1} f^{(n)}(\tau) d\tau, & n-1 < \kappa < n, n \in \mathbb{N}. \end{cases} \quad (2)$$

Definition 3. The Mittag-Leffler function with one operator is defined as follows [1]:

$$E_\kappa(z) = \sum_{\varsigma=0}^{\infty} \frac{z^\varsigma}{\Gamma(\kappa\varsigma + 1)}, \kappa > 0, z \in \mathbb{C}. \quad (3)$$

3. Model Description

To illustrate the dynamics of the yeast prion system, we have modified the bi-stable mathematical model that Lemarre et al. [31] first proposed. In particular, we have altered the model by adding various population degeneration rates. The variable $N(t)$ shows the concentration of soluble Sup35 at time t , while $P(t)$ describes the concentration of Sup35 prions at time t . The following system of ordinary differential equations describes the model, which is shown in Figure 1.

$$\begin{aligned} \frac{dN(t)}{dt} &= \alpha - \beta N(t) - \delta N(t)f(P(t)), \\ \frac{dP(t)}{dt} &= \delta N(t)f(P(t)) - \lambda P(t), \end{aligned} \quad (4)$$

where

$$f(P(t)) = \frac{P(t)^2}{\kappa^2 + P(t)^2}.$$

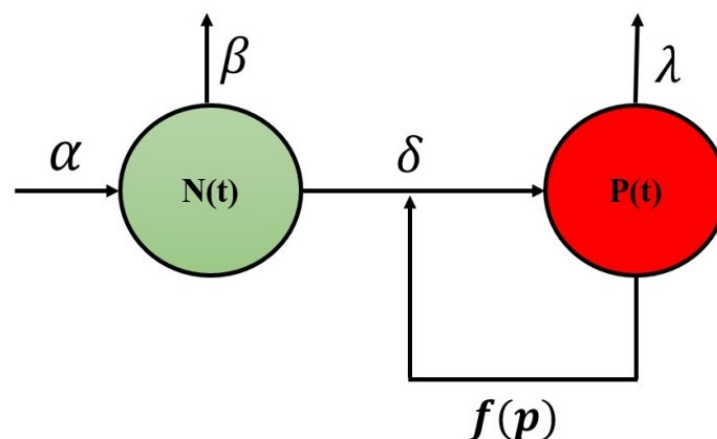


Figure 1. The schematic diagram of the above-described model (4).

Initial conditions $N(0) = C_1$ and $P(0) = C_2$ are taken into consideration. The function $f(P)$ is selected to be a Hill function because it has the unique property of making the system multi-stable. The model that is being studied can be expressed in the Caputo fractional derivative as follows. Table 1 lists all of the system's parameters and their corresponding values.

$$\begin{aligned} {}^C D_t^\eta N(t) &= \alpha - \beta N(t) - \frac{\delta N(t)P(t)^2}{\kappa^2 + P(t)^2}, \\ {}^C D_t^\eta P(t) &= \frac{\delta N(t)P(t)^2}{\kappa^2 + P(t)^2} - \lambda P(t). \end{aligned} \quad (5)$$

Table 1. A description of the parameters and their values shown in the suggested system (4) [31].

Parameters	Descriptions	Values
α	Growth rate of Sup35 monomers	0.7
β	Degeneration rate of Sup35 monomers	0.06
δ	Rate of conversion from monomer to prion aggregates	10
λ	Degeneration rate of Sup35 prions	0.13
κ	Threshold parameter	2

4. Existence and Uniqueness Analysis

We simplify model (5) as follows in order to prove its existence and uniqueness.

$$\begin{aligned} {}^C D_t^\eta N(t) &= H_1(t, N), \\ {}^C D_t^\eta P(t) &= H_2(t, P). \end{aligned} \quad (6)$$

Initial conditions are $N(0) = N_0$ and $P(0) = P_0$. Here, ${}^C D_t^\eta$ symbolizes the Caputo fractional derivative of order η . Using facts of fixed point theory, we prove the existence of a unique solution for the fractional yeast prion model.

Consider

$${}^C D_t^\eta N(t) = H_1(t, N), t \in [0, T], 0 < \eta \leq 1, \quad (7)$$

subjected to the initial condition

$$N(0) = N_0, \quad (8)$$

where $H_1 : [0, T] \times \mathbb{R}^n \times \mathbb{R}^n \rightarrow \mathbb{R}^n$ is continuous and $N \in \mathbb{R}^n$, $T > 0$.

Here, \mathbb{R}^n is the Euclidean space described by the norm $\|\cdot\|$ that has n -dimensions.

We present the analysis for N , the remaining equation in system (6) will behave in a comparable way.

Lemma 1 ([32]). *The space of continuous function which is represented by $N \in C([0, T]; \mathbb{R})$ and $N : [0, T] \rightarrow \mathbb{R}$ having a sub norm $\|\cdot\|_\infty$ is an outcome of the above-mentioned problem (7) and (8) on the interval $[0, T]$ if and only if it is a solution of the Volterra integral equation*

$$N(t) = N(0) + \frac{1}{\Gamma(\eta)} \int_0^t (t - \xi)^{\eta-1} H_1(\xi, N) d\xi, \quad \forall t \in [0, T]. \quad (9)$$

Theorem 1. (Existence) *Let us consider that $0 < \eta \leq 1$, $N_0 \in \mathbb{R}$, $T^* > 0$ and $X > 0$. Derive $H := \{(t, N) : t \in [0, T^*], |N - N_0| \leq X\}$ and considering that the mapping $H_1 : H \rightarrow \mathbb{R}$ is continuous. Additionally, defining $Y := \sup_{(t, N, P) \in G} |H_1(t, N)|$ and*

$$T = \begin{cases} T^*, & \text{if } Y = 0, \\ \min \left\{ T^*, \left(\frac{X\Gamma(\eta+1)}{Y} \right)^{\frac{1}{\eta}} \right\}, & \text{otherwise.} \end{cases} \quad (10)$$

Following that, the initial value problems (7) and (8) can be resolved by a function called $N \in C[0, T]$.

Proof. If $Y = 0$ then $H_1(t, N) = 0 \quad \forall (t, N) \in H$. In the present case, direct substitution makes it evident that the function $N : [0, T] \rightarrow \mathbb{R}$ having $N(t) = N_0$ provides a solution to the problem under consideration. Therefore, there is a solution in this case [33,34].

Describe the set $S := \{N \in C[0, T] : \|N - N_0\| \leq X\}$. Knowing the Chebyshev norm, it is evident that S is a convex and also closed subset of all continuous functions on $[0, T]$ in Banach space. For $Y \neq 0$, we prove that (7) and (8) is equal to Equation (9), which is the Volterra integral. Therefore, Banach space is S since $N_0 \in S$, S is non-empty. On this set S , the operator E is defined by

$$(EN)(t) := N(0) + \frac{1}{\Gamma(\eta)} \int_0^t (t - \xi)^{\eta-1} H_1(\xi, N) d\xi, \quad \forall t \in [0, T] \quad (11)$$

Since $N = EN$ can thus be used to write the Volterra Equation (9) and consequently, the Schauders Second Fixed-Point Theorem can be employed to demonstrate that E contains a fixed point. Now, we demonstrate that S is closed, implying that $EN \in S$ for $N \in S$. Now, we notice that in the case of $0 \leq t_1 \leq t_2 \leq T$.

$$\begin{aligned} |(EN)(t_1) - (EN)(t_2)| &= \frac{1}{\Gamma(\eta)} \left| \int_0^{t_1} (t_1 - \xi)^{\eta-1} H_1(\xi, N) d\xi - \int_0^{t_2} (t_2 - \xi)^{\eta-1} H_1(\xi, N) d\xi \right| \\ &= \frac{1}{\Gamma(\eta)} \left| \int_0^{t_1} [(t_1 - \xi)^{\eta-1} - (t_2 - \xi)^{\eta-1}] H_1(\xi, N) d\xi + \int_{t_1}^{t_2} (t_2 - \xi)^{\eta-1} H_1(\xi, N) d\xi \right| \\ &\leq \frac{Y}{\Gamma(\eta)} \left(\int_0^{t_1} |(t_1 - \xi)^{\eta-1} - (t_2 - \xi)^{\eta-1}| d\xi + \int_{t_1}^{t_2} (t_2 - \xi)^{\eta-1} d\xi \right) \end{aligned}$$

The value of the second integral in the previous inequality's right side is $(t_2 - \xi)^\eta$. Consider the two cases for the first integral $\eta < 1$, $\eta = 1$, separately. When $\eta = 1$, the integral is equal to zero. There is $(t_2 - \xi)^{\eta-1} \leq (t_1 - \xi)^{\eta-1}$ for $\eta < 1$.

Thus,

$$\begin{aligned} \int_0^{t_1} |(t_1 - \xi)^{\eta-1} - (t_2 - \xi)^{\eta-1}| d\xi &= \int_0^{t_1} [(t_1 - \xi)^{\eta-1} - (t_2 - \xi)^{\eta-1}] d\xi \\ &= (t_2 - t_1)^\eta + (t_1^\eta - t_2^\eta) \\ &\leq (t_2 - t_1)^\eta. \end{aligned}$$

When we combine these findings, we obtain

$$|(EN)(t_1) - (EN)(t_2)| \leq \frac{2Y}{\Gamma(\eta + 1)} (t_2 - t_1)^\eta \quad (12)$$

The expression in (12) that is on the right-hand side converges to zero in either case when $t_2 \rightarrow t_1$. Therefore, knowing that $N(0)$ is continuous, it shows that EN is continuous function. For $N \in S$ and $t \in [0, T]$, it is equally true.

$$\begin{aligned} |(EN)(t_1) - N(0)| &= \frac{1}{\Gamma(\eta)} \left| \int_0^t (t - \xi)^{\eta-1} H_1(\xi, N) d\xi \right| \\ &\leq \frac{Y}{\Gamma(\eta+1)} t^\eta \leq \frac{Y}{\Gamma(\eta+1)} T^\eta \\ &\leq \frac{Y}{\Gamma(\eta+1)} \cdot \frac{X\Gamma(\eta+1)}{Y} = X. \end{aligned} \quad (13)$$

Therefore, if $N \in S$, then we have $EN \in S$. Specifically, the set S is mapped onto itself. Next, we have to show that $E(S) := \{Es : s \in S\}$ is compact. So that this is achieved with the aid of the Arzel'a–Ascoli Theorem. Let us consider $z \in E(S)$ to prove that $E(S)$ is a uniformly bounded set. For every $t \in [0, T]$, we observe that

$$\begin{aligned} |z(t)| &= |(EN)(t)| \\ &\leq \|N(0)\|_\infty + \frac{1}{\Gamma(\eta)} \int_0^t (t - \xi)^{\eta-1} |H_1(\xi, N)| d\xi \\ &\leq \|N(0)\|_\infty + \frac{1}{\Gamma(\eta+1)} Y T^\eta \leq \|N(0)\|_\infty + X. \end{aligned}$$

This is the necessary boundedness property. It is easy to derive the property of equicontinuity from (12). We proved in the case $\eta \leq 1$ for $0 \leq t_1 \leq t_2 \leq T$ that

$$|(EN)(t_1 - t_2)| \leq \frac{2Y}{\Gamma(\eta+1)} (t_2 - t_1)^\eta.$$

Following the use of the Mean Value Theorem and the Triangular Inequality, we obtain

$$\begin{aligned} |(EN)(t_1) - (EN)(t_2)| &\leq \frac{2Y}{\Gamma(\eta+1)} (t_2 - t_1)^\eta \\ |(EN)(t_1) - (EN)(t_2)| &\leq \frac{2Y}{\Gamma(\eta+1)} (t_2 - t_1)^\eta \end{aligned}$$

Therefore, if $|t_1 - t_2| < \chi$, we obtain

$$|(EN)(t_1) - (EN)(t_2)| \leq Y'\chi + \frac{2Y}{\Gamma(\eta+1)} \chi^\eta T^\eta.$$

$N(0)$ is uniformly continuous between $[0, T]$. We may observe that the set $E(S)$ is equicontinuous since the right side statement is not dependent on t_1, t_2 and N . In either case, the Schauders Second Fixed-Point Theorem states there is a fixed point that exists in E since the above-mentioned theorem called the Arzel'a–Ascoli Theorem gives $E(S)$ that is compact. For Equations (7) and (8), this fixed point is the necessary result.

We now address the unique results. First, we observe that operator E has the following properties. Thus, let $N_1, N_2 \in C[0, T] \subset [0, t]$ while a constant $\phi > 0$ exists that is independent of t, N_1 and N_2 such that $|H_1(t, N_1) - H_1(t, N_2)| \leq \phi|N_1 - N_2|$ for all $t \in [0, T]$. Then, we receive

$$\|EN_1 - EN_2\|_{L^\infty[0, t]} = \frac{1}{\Gamma(\mu)} \sup_{0 \leq \tau \leq t} \left| \int_0^\tau (\tau - \xi)^{\eta-1} [H_1(\xi, N_1) - H_1(\xi, N_2)] d\xi \right|$$

$$\begin{aligned}
&\leq \frac{\phi}{\Gamma(\eta)} \sup_{0 \leq \tau \leq t} \left| \int_0^\tau (\tau - \xi)^{\eta-1} |N_1(\xi) - N_2(\xi)| d\xi \right| \\
&\leq \frac{\phi}{\Gamma(\eta)} \|N_1 - N_2\|_{L_\infty[0,t]} \sup_{0 \leq \tau \leq t} \left| \int_0^\tau (\tau - \xi)^{\eta-1} d\xi \right| \\
&\leq \frac{\phi}{\Gamma(\eta)} \|N_1 - N_2\|_{L_\infty[0,t]} \sup_{0 \leq \tau \leq t} |(\tau - \xi)^\eta|_0^\tau \\
&= \frac{\phi}{\Gamma(\eta + 1)} \|N_1 - N_2\|_{L_\infty[0,t]}.
\end{aligned}$$

□

Theorem 2. (Uniqueness) Assume $N(0) \in \mathbb{R}$, $X > 0$ and $T^* > 0$. Also consider $0 < \eta \leq 1$ and $\varepsilon = \lceil \eta \rceil$. Consider the mapping $H_1 : H \rightarrow \mathbb{R}$ be continuous and adheres to the Lipschitz constraints with regard to the second variable, i.e.,

$$|Y_1(t, T_{I_1}) - Y_1(t, T_{I_2})| \leq \eta |T_{I_1} - T_{I_2}|,$$

for some constants $\phi > 0$ independent of t , N_1 and N_2 . Then, the initial value problems (7) and (8) have a unique solution $N \in C[0, T]$.

Proof. According to the above theorem, the problems (7) and (8) under consideration have a solution. Now we have to show the uniqueness [33,34]. Specifically, using the operator E from Equation (11) we find that it maps the nonempty, closed and convex set $S = \{N \in C[0, T] : \|N - N_0\|_\infty \leq X\}$ to itself. In order to demonstrate E possesses a fixed point which is unique, we employ Weissingers Fixed Point Theorem. Let $j \in \mathbb{N}_0$, $t \in [0, T]$ and $N_1, N_2 \in S$. Next, using the norm called Chebyshev norms on the interval $[0, T]$ and applying (15) to the result, we obtain

$$\|E^j N - E^j N'\|_\infty \leq \|N - N'\|_\infty \frac{\phi^j}{\Gamma(\eta j + 1)}$$

Let $\tau_j = \phi^j / \Gamma(\eta j + 1)$. Proving the convergence of the series $\sum_{j=0}^{\infty} \tau_j$ is all that is required to apply the theorem. It is evident that the Mittag-Leffler function is only represented by a power series E_η^* and the series converges as a result. This brings the proof to the end. □

5. Stability Analysis

If we set the right-hand side of Equation (5) to zero, we can obtain the equilibrium points of the fractional yeast prion model.

$${}^C D_t^\eta N(t) = {}^C D_t^\eta P(t) = 0. \quad (14)$$

Therefore,

$$\begin{aligned}
\alpha - \beta N(t) - \frac{\delta N(t) P(t)^2}{\kappa^2 + P(t)^2} &= 0, \\
\frac{\delta N(t) P(t)^2}{\kappa^2 + P(t)^2} - \lambda P(t) &= 0.
\end{aligned} \quad (15)$$

We find the equilibrium points by solving (15),

- Prion-free equilibrium Point: $E_1 = \left(\frac{\alpha}{\beta}, 0\right) = (11.6666, 0)$.
- $E_2 = \left(\frac{\alpha(2\beta + \lambda) + \lambda\sqrt{\alpha^2 - 4\beta\kappa^2(\beta + \lambda)}}{2\beta(\beta + \lambda)}, \frac{\alpha - \sqrt{\alpha^2 - 4\beta\kappa^2(\beta + \lambda)}}{2(\beta + \lambda)}\right) = (10.8377, 0.382587)$.

$$\bullet \quad E_3 = \left(\frac{\alpha(2\beta+\lambda) - \lambda\sqrt{\alpha^2 - 4\beta\kappa^2(\beta+\lambda)}}{2\beta(\beta+\lambda)}, \frac{\alpha + \sqrt{\alpha^2 - 4\beta\kappa^2(\beta+\lambda)}}{2(\beta+\lambda)} \right) = (4.51315, 3.30162).$$

For the model under consideration, the Jacobian matrix J is as follows

$$J = \begin{bmatrix} -\beta - \frac{\delta P(t)^2}{\kappa^2 + P(t)^2} & -\delta N(t) \left(\frac{(\kappa^2 + P(t)^2)2P(t) - 2P(t)^3}{(\kappa^2 + P(t)^2)^2} \right) \\ \frac{\delta P(t)^2}{\kappa^2 + P(t)^2} & -\delta N(t) \left(\frac{(\kappa^2 + P(t)^2)2P(t) - 2P(t)^3}{(\kappa^2 + P(t)^2)^2} \right) - \lambda \end{bmatrix}$$

The following is the Jacobian matrix J at the Prion-free equilibrium point:

$$J_1 = \begin{bmatrix} -0.06 & 0 \\ 0 & -0.13 \end{bmatrix}$$

The eigenvalues corresponding to the matrix J_1 are $\omega_{11} = -0.13$, $\omega_{12} = -0.06$.

The Jacobian matrix J at the equilibrium point E_2 is given as follows:

$$J_2 = \begin{bmatrix} -0.0645892 & -0.250821 \\ 0.00458918 & -0.380821 \end{bmatrix}$$

The eigenvalues corresponding to the above matrix are $\omega_{21} = -0.377138$, $\omega_{22} = -0.068272$.

At the equilibrium point E_3 , the Jacobian matrix is as follows:

$$J_3 = \begin{bmatrix} -0.155102 & -0.0697955 \\ 0.0951023 & -0.199795 \end{bmatrix}$$

In accordance with the above matrix, the eigenvalues are

$$\omega_{31} = -0.0991014, \omega_{32} = -0.2557966.$$

Since each and every eigenvalue is negative, the system under investigation is stable. The model's asymptotic result is dependent on the initial condition in cases where all three equilibrium points exist. In contrast, if the initial concentration of aggregates is sufficient, their population will be steadily maintained. If the concentration of aggregates is too low, the solution will converge to the prion-free equilibrium.

6. Solution of the Model Using PC Scheme

The PC method is a developed version of the classical trapezoidal rule that we will now review. This approach's success has been proven by numerous examples of real-world applications. In order to obtain the solution of the predicted model, we here apply the PC approach [28].

Let us consider the fractional order yeast prion model of the differential equation

$${}^C D_t^\eta [N(t)] = H_1(t, N), \quad t \in [0, T], \quad 0 < \eta \leq 1, \quad (16)$$

$$N(t) = C_1. \quad (17)$$

Let us think about a uniform grid $\{t_m = mh : m = -n, (-n) + 1, (-n) + 2, \dots, -1, 0, 1, \dots, \mathbb{N}\}$ and $h = \frac{T}{\mathbb{N}}$, where \mathbb{N} is the set of natural numbers and n are integers.

$$N_h(t_i) = C_1, \quad i = -n, -n + 1, -n + 2, \dots, -1, 0. \quad (18)$$

$N_h(t_i) \approx N(t_i)$, ($i = -n, -n+1, -n+2, \dots, -1, 0, 1, \dots, m$) and we would like to evaluate $N_h(t_{m+1})$ using the Volterra integral equation, which corresponds to Equations (16) and (17). Assuming that the approximations have been computed already.

$$N(t_{m+1}) = N(0) + \frac{1}{\Gamma(\eta)} \int_0^{t_{m+1}} (t_{m+1} - \xi)^{\eta-1} H_1(\xi, N(\xi)) d\xi. \quad (19)$$

In Equation (19), we utilize approximations $N_h(t_m)$ for $N(t_m)$. Moreover, the integral is computed using the product trapezoidal quadrature formula in Equation (19). Thus, the corrector formula is

$$N_h(t_{m+1}) = N(0) + \frac{h^\eta}{\Gamma(\eta+2)} H_1(t_{m+1}, N_h(t_{m+1})) + \frac{h^\eta}{\Gamma(\eta+2)} \sum_{i=0}^m a_{i,m+1} H_1(t_i, N_h(t_i)), \quad (20)$$

where

$$a_{i,m+1} = \begin{cases} m^{\eta+1} - (m-\eta)(m+1)^\eta, & i=0 \\ (m-i+2)^{\eta+1} - 2(m-i+1)^{\eta+1} + (m-i)^{\eta+1}, & 1 \leq i \leq m \\ 1, & i=m+1 \end{cases} \quad (21)$$

The unknown $N_h(t_{m+1})$ term is present on both sides of Equation (20). It is not possible to answer Equation (20) explicitly for $N_h(t_{m+1})$ due to the nonlinearity of H_1 . Therefore, we replace the $N_h(t_{m+1})$ term on the right side with an estimate $N_h^p(t_{m+1})$, which is known as the predictor. The product rectangle rule is used in Equation (20) to evaluate the predictor term.

$$N_h^p(t_{m+1}) = N(0) + \frac{1}{\Gamma(\eta)} \sum_{i=0}^m b_{i,m+1} H_1(t_i, N_h(t_i)). \quad (22)$$

Here

$$b_{i,m+1} = \frac{h^\eta}{\eta} ((m-i+1)^\eta - (m-i)^\eta). \quad (23)$$

For both systems of Equation (6), the corrector formulas are thus as follows, derived from the computations carried out above:

$$\begin{aligned} N_h(t_{m+1}) &= N(0) + \frac{h^\eta}{\Gamma(\eta+2)} H_1(t_{m+1}, N_h(t_{m+1})) + \frac{h^\eta}{\Gamma(\eta+2)} \sum_{i=0}^m a_{i,m+1} H_1(t_i, N_h(t_i)), \\ P_h(t_{m+1}) &= P(0) + \frac{h^\eta}{\Gamma(\eta+2)} H_2(t_{m+1}, P_h(t_{m+1})) + \frac{h^\eta}{\Gamma(\eta+2)} \sum_{i=0}^m a_{i,m+1} H_2(t_i, P_h(t_i)). \end{aligned} \quad (24)$$

In the same way, the predictor terms are

$$\begin{aligned} N_h^p(t_{m+1}) &= N(0) + \frac{1}{\Gamma(\eta)} \sum_{i=0}^m b_{i,m+1} H_1(t_i, N_h(t_i)), \\ P_h^p(t_{m+1}) &= P(0) + \frac{1}{\Gamma(\eta)} \sum_{i=0}^m b_{i,m+1} H_2(t_i, P_h(t_i)). \end{aligned} \quad (25)$$

Here is the considered system of equations for different fractional-order yeast prion models.

$$\begin{aligned} {}^C D_t^\eta N(t) &= \alpha - \beta N(t) - \frac{\delta N(t) P(t)^2}{\kappa^2 + P(t)^2}, \\ {}^C D_t^\mu P(t) &= \frac{\delta N(t) P(t)^2}{\kappa^2 + P(t)^2} - \lambda P(t). \end{aligned} \quad (26)$$

Now, the following graphs are the solutions of $N(t)$ and $P(t)$ under various combinations of fractional orders η and μ . When the fractional orders have different values, the prion population increases and the monomer population decreases.

7. Results and Discussion

Using the numerical data from Table 1, we programmed Mathematica to perform graphical simulations for the obtained PC approach solutions (24) and (25). Figures 2 and 3 depict the nature of the results produced by the suggested solution strategy for $N(t)$ and $P(t)$ in relation to time for different values of fractional order.

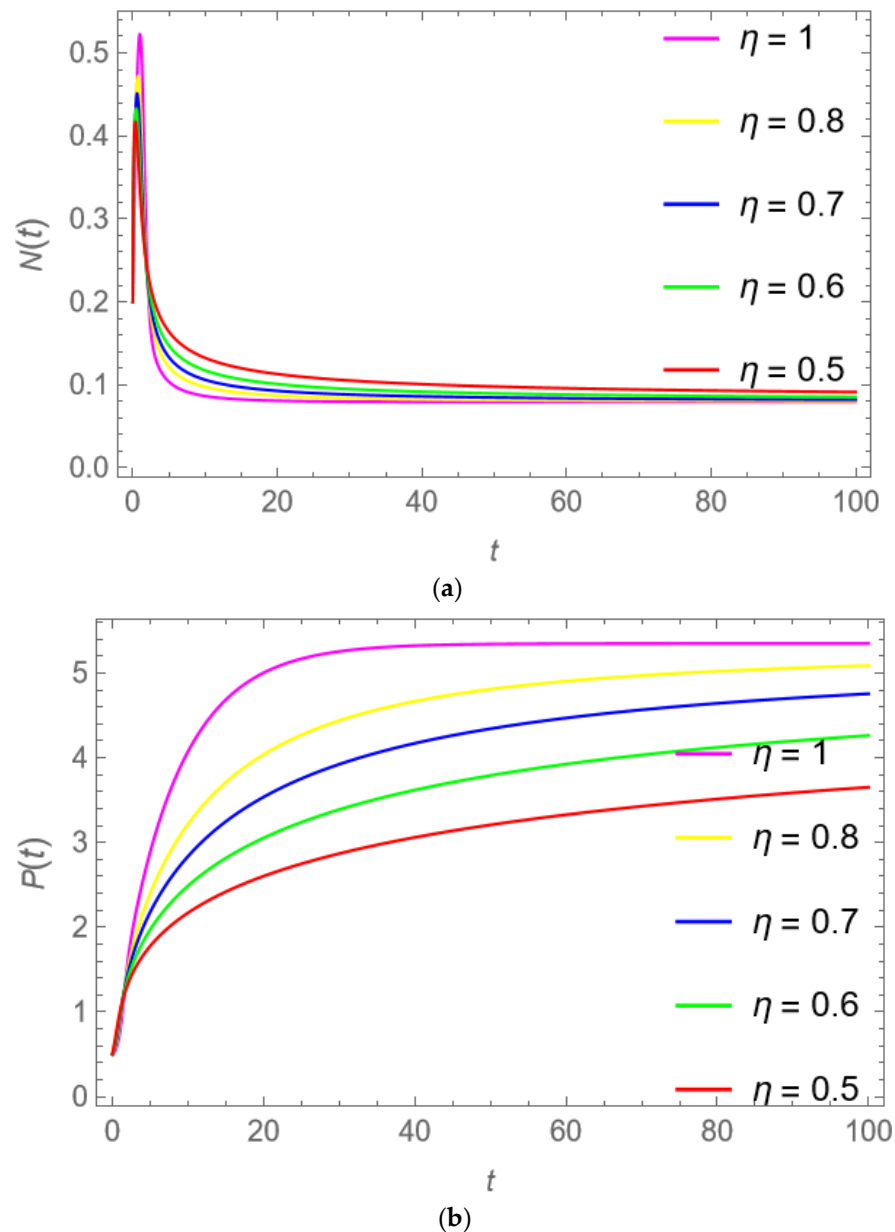


Figure 2. (a): Nature of solution of the concentration of Sup35 $N(t)$ for different fractional orders $\eta = 1, 0.8, 0.7, 0.6, 0.5$. (b): Solution plot of Sup35 concentration in prion conformation $P(t)$ with different fractional orders $\eta = 1, 0.8, 0.7, 0.6, 0.5$.

Figure 2a,b show the solutions $N(t)$ and $P(t)$ of the yeast prion system, respectively. Five distinct values of η , that is, $\eta = 0.5, 0.6, 0.7, 0.8$ and 1 have been taken into consideration for each illustration. The solutions $N(t)$ and $P(t)$ under various combinations of values for both η and μ are plotted in Figure 3. Figure 3i illustrates how each solution curve $N(t)$ reaches its maximum point faster over time t and then rapidly falls as the values of the fractional order η grow (for fixed $\mu = 1$). Maximum Sup35 monomer density increases with increasing μ (for fixed $\eta = 1$) along time t as seen in Figure 3iii and then decreases.

In Figure 3ii,iv, as fractional orders (η and μ respectively) grow, all of the solution curves $P(t)$ first decline with respect to one another. However, after a while, all of the curves begin to increase within the time frame. The theory of prion generation and propagation can be demonstrated with the yeast prion system. A valuable tool for understanding the characteristics of human amyloidogenic proteins is the yeast prion system. Numerous fields benefit greatly from the study of fractional-order differential equations and the application of PC when examining complicated dynamical systems.

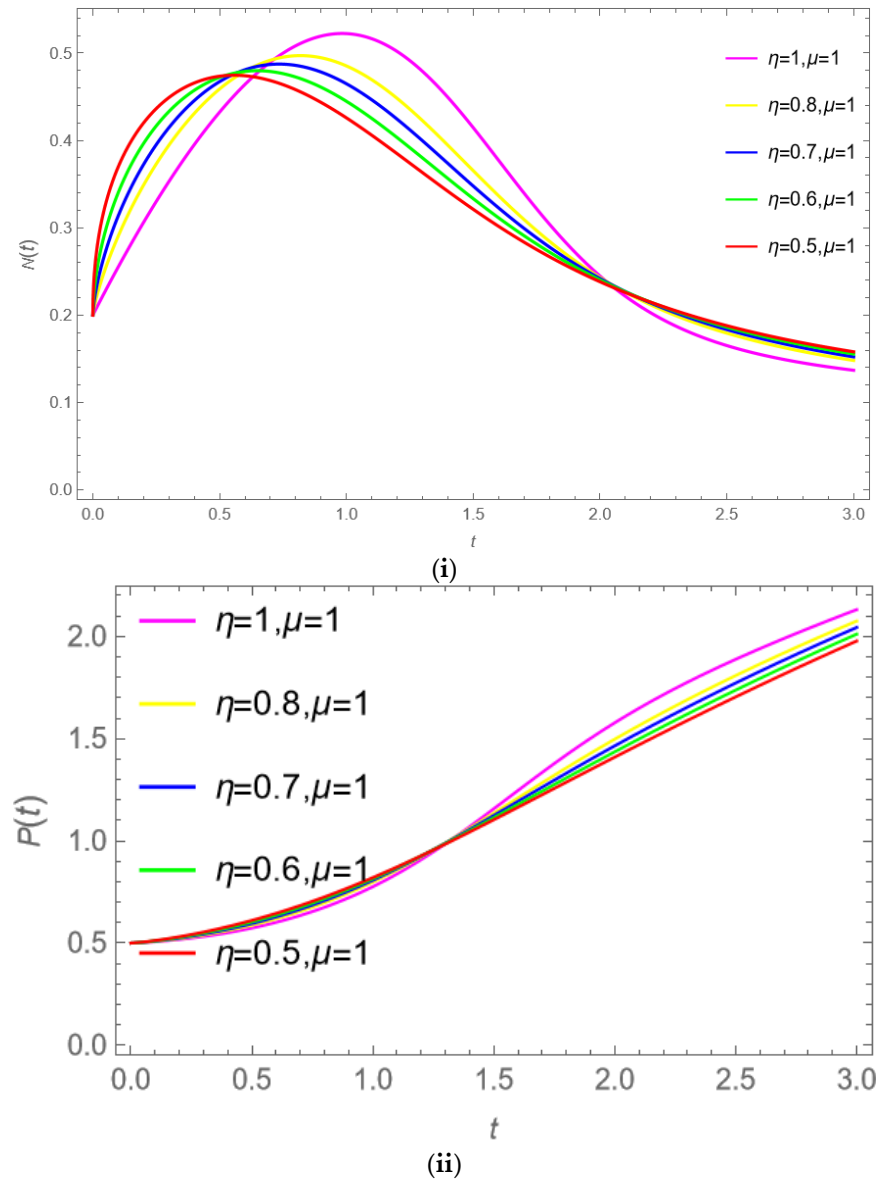


Figure 3. Cont.

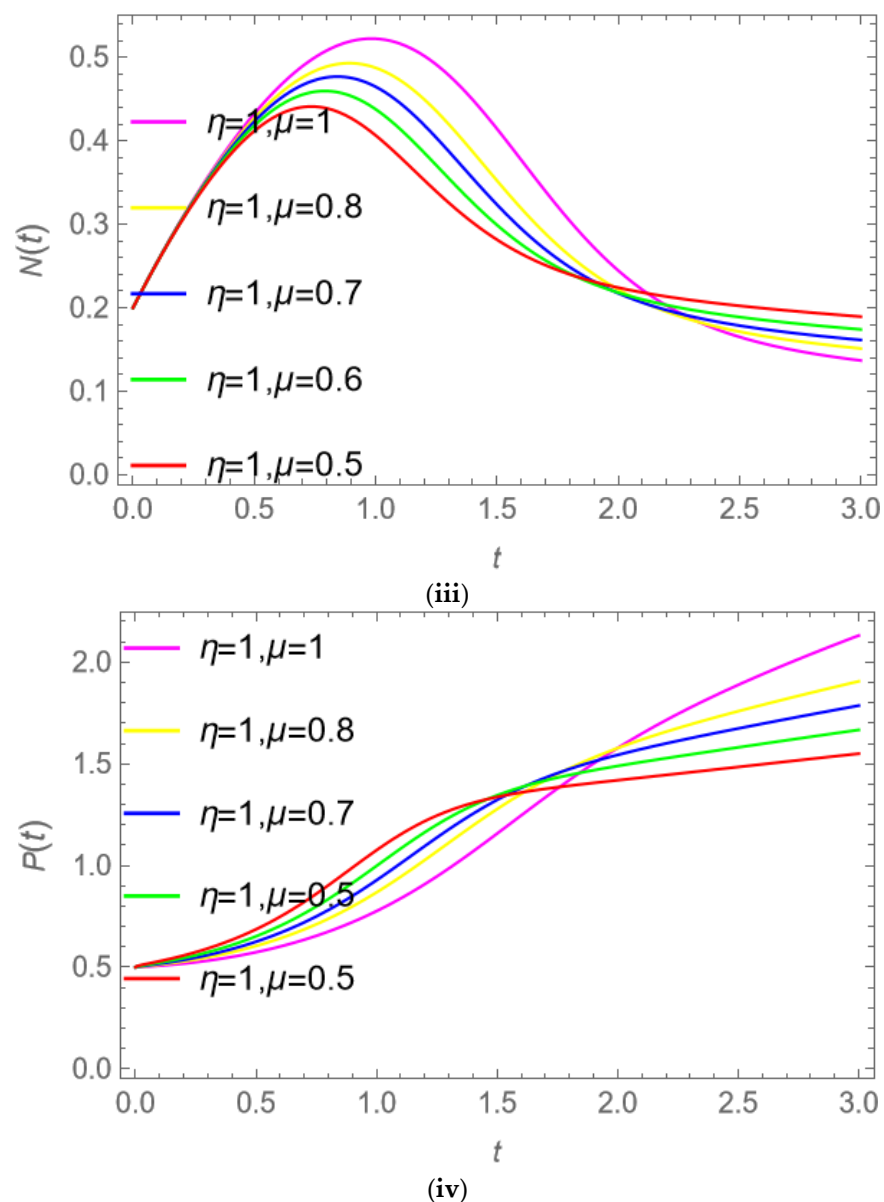


Figure 3. (i–iv): The graphs showing solutions of the system (26) for time t for both fixed and variable fractional order values.

8. Conclusions

This work evaluates a yeast prion model that includes a Sup35 monomer and Sup35 prion. We performed stability analysis by finding the equilibrium points as well as the uniqueness and existence of the model. Both analyses exhibit the qualitative behaviour of the suggested model. Required solutions are computed for the given model using the Caputo fractional derivative and the preferred approach. Different graphical results for the solution of the system with different fractional order levels have been presented. Also, the graphs that are given show that when the fractional orders have different values, the prion population increases, and the monomer population decreases. This paper presents illustrations that highlight the contribution of fractional derivatives to the result. In many fields, the study of fractional-order differential equations and the use of the PC approach can be very helpful in the analysis of complicated dynamical systems. We address the current and future studies on neurodegenerative diseases as well as the paradigm shifts in disease description and diagnosis. Neurodegenerative disease descriptive epidemiology is changing quickly. The

future planning and results of population-based research as well as the formulation of public health intervention policy will be enhanced by these implementations.

Author Contributions: Conceptualization, D.K.A. and D.G.P.; methodology, D.K.A.; software D.K.A.; validation, D.K.A., D.G.P. and N.B.T.; formal analysis, D.K.A.; investigation, D.G.P.; resources, N.B.T.; data curation, N.B.T.; writing—original draft preparation D.K.A.; writing—review and editing, D.G.P. and N.B.T.; visualization, N.B.T.; supervision, D.G.P.; project administration, D.G.P. All authors have read and agreed to the published version of the manuscript.

Funding: This project was supported by the Researchers Supporting Project number (RSP2024R413), King Saud University, Riyadh, Saudi Arabia.

Data Availability Statement: The original contributions presented in the study are included in the article, further inquiries can be directed to the corresponding author.

Acknowledgments: Authors are thankful to the reviewers for their valuable suggestions in improving the paper.

Conflicts of Interest: The authors declare no conflicts of interest.

References

- Podlubny, I. *Fractional Differential Equations*; Academic Press: New York, NY, USA, 1999.
- Ross, B. The Development of Fractional Calculus 1695–1900. *Hist. Math.* **1977**, *4*, 75–89. [[CrossRef](#)]
- Caputo, M. *Elasticità e Dissipazione*; Zanichelli: Bologna, Italy, 1969.
- Miller, K.S.; Ross, B. *An Introduction to Fractional Calculus and Fractional Differential Equations*; Wiley: New York, NY, USA, 1993.
- Caputo, M. Linear Models of Dissipation Whose Q Is Almost Frequency Independent—II. *Geophys. J. Int.* **1967**, *13*, 529–539. [[CrossRef](#)]
- Veerasha, P.; Prakasha, D.G. An Efficient Technique for Two-Dimensional Fractional Order Biological Population Model. *Int. J. Model. Simul. Sci. Comput.* **2020**, *11*, 2050005. [[CrossRef](#)]
- Kumar, S.; Kumar, D.; Singh, J. Numerical Computation of Fractional Black–Scholes Equation Arising in Financial Market. *Egypt. J. Basic Appl. Sci.* **2014**, *1*, 177–183. [[CrossRef](#)]
- Barbero, G.; Evangelista, L.R.; Zola, R.S.; Lenzi, E.K.; Scarfone, A.M. A Brief Review of Fractional Calculus as a Tool for Applications in Physics: Adsorption Phenomena and Electrical Impedance in Complex Fluids. *Fractal Fract.* **2024**, *8*, 369. [[CrossRef](#)]
- Logeswari, K.; Ravichandran, C.; Nisar, K.S. Mathematical Model for Spreading of COVID-19 Virus with the Mittag–Leffler Kernel. *Numer. Methods Partial. Differ. Equ.* **2020**, *40*, e22652. [[CrossRef](#)]
- Baleanu, D.; Guvenc, Z.B.; Machado, J.A.T. *New Trends in Nanotechnology and Fractional Calculus Applications*; Springer: Berlin/Heidelberg, Germany, 2010; Volume 10, pp. 978–990.
- Kumar, D.; Seadawy, A.R.; Joardar, A.K. Modified Kudryashov Method via New Exact Solutions for Some Conformable Fractional Differential Equations Arising in Mathematical Biology. *Chin. J. Phys.* **2018**, *56*, 75–85. [[CrossRef](#)]
- Koleva, M.N.; Vulkov, L.G. A Quasilinearization Approach for Identification Control Vectors in Fractional-Order Nonlinear Systems. *Fractal Fract.* **2024**, *8*, 196. [[CrossRef](#)]
- Kumar, S.; Kumar, D.; Abbasbandy, S.; Rashidi, M.M. Analytical Solution of Fractional Navier–Stokes Equation by Using Modified Laplace Decomposition Method. *Ain Shams Eng. J.* **2014**, *2*, 569–574. [[CrossRef](#)]
- Agarwal, P.; El-Sayed, A.A. Non-Standard Finite Difference and Chebyshev Collocation Methods for Solving Fractional Diffusion Equation. *Phys. Stat. Mech. Appl.* **2018**, *500*, 40–49. [[CrossRef](#)]
- Angiulli, G.; Versaci, M.; Calcagno, S. Computation of the Cutoff Wavenumbers of Metallic Waveguides with Symmetries by Using a Nonlinear Eigenproblem Formulation: A Group Theoretical Approach. *Mathematics* **2020**, *8*, 489. [[CrossRef](#)]
- Veerasha, P.; Prakasha, D.G.; Baleanu, D. Analysis of Fractional Swift–Hohenberg Equation Using a Novel Computational Technique. *Math. Methods Appl. Sci.* **2020**, *43*, 1970–1987. [[CrossRef](#)]
- Kumar, D.; Nama, H.; Singh, J.; Kumar, J. An Efficient Numerical Scheme for Fractional Order Mathematical Model of Cytosolic Calcium Ion in Astrocytes. *Fractal Fract.* **2024**, *8*, 184. [[CrossRef](#)]
- Angiulli, G.; Versaci, M.; Morabito, F.C. Computation of Nonlinear Eigenvalues Related to Parameters of Microwave Structures by Using Group Theory. In Proceedings of the 2017 International Applied Computational Electromagnetics Society Symposium—Italy (ACES), Firenze, Italy, 26–30 March 2017; pp. 1–2.
- Davis, J.K.; Sindi, S.S. A Mathematical Model of the Dynamics of Prion Aggregates with Chaperone-Mediated Fragmentation. *J. Math. Biol.* **2016**, *72*, 1555–1578. [[CrossRef](#)] [[PubMed](#)]
- Borgqvist, J.G.; Alexandersen, C.G. HeMiTo-Dynamics: A Characterisation of Mammalian Prion Toxicity Using Non-Dimensionalisation, Linear Stability and Perturbation Analyses. *arXiv* **2024**, arXiv:2405.10070.
- Kushnirov, V.V.; Dergalev, A.A.; Alieva, M.K.; Alexandrov, A.I. Structural Bases of Prion Variation in Yeast. *Int. J. Mol. Sci.* **2022**, *23*, 5738. [[CrossRef](#)] [[PubMed](#)]

22. Norton, J.; Seah, N.; Santiago, F.; Sindi, S.; Serio, T. Multiple Aspects of Amyloid Dynamics In Vivo Integrate to Establish Prion Variant Dominance in Yeast. *Front. Mol. Neurosci.* **2024**, *17*, 1439442. [[CrossRef](#)]
23. Wickner, R.B.; Edskes, H.K.; Wu, S.; Gregg, K. Prions Are the Greatest Protein Misfolding Problem, and Yeast Has Several Solutions. *PLoS Pathog.* **2023**, *19*, e1011333. [[CrossRef](#)] [[PubMed](#)]
24. Chernoff, Y.O.; Grizel, A.V.; Rubel, A.A.; Zelinsky, A.A.; Chandramowlishwaran, P.; Chernova, T.A. Application of yeast to studying amyloid and prion diseases. *Adv. Genet.* **2020**, *105*, 293–380.
25. Miller, E.M.; Chan, T.C.D.; Montes-Matamoros, C.; Sharif, O.; Pujo-Menjouet, L.; Lindstrom, M.R. Oscillations in Neuronal Activity: A Neuron-Centered Spatiotemporal Model of the Unfolded Protein Response in Prion Diseases. *Bull. Math. Biol.* **2024**, *86*, 82. [[CrossRef](#)]
26. Elettrey, M.; Ahmed, E.; Alqahtani, A. A Discrete Fractional-Order Prion Model Motivated by Parkinson's Disease. *Math. Probl. Eng.* **2020**, *2020*, 4308589. [[CrossRef](#)]
27. Veerasha, P. The Efficient Fractional Order Based Approach to Analyze Chemical Reaction Associated with Pattern Formation. *Chaos Solitons Fractals* **2022**, *165*, 112862. [[CrossRef](#)]
28. Kumar, P.; Saat Erturk, V. The Analysis of a Time Delay Fractional COVID-19 Model via Caputo Type Fractional Derivative. *Math. Methods Appl. Sci.* **2023**, *46*, 7618–7631. [[CrossRef](#)] [[PubMed](#)]
29. Odibat, Z. A Universal Predictor–Corrector Algorithm for Numerical Simulation of Generalized Fractional Differential Equations. *Nonlinear Dyn.* **2021**, *105*, 2363–2374. [[CrossRef](#)]
30. Ameen, I.G.; Sweilam, N.H.; Ali, H.M. A Fractional-Order Model of Human Liver: Analytic-Approximate and Numerical Solutions Comparing with Clinical Data. *Alex. Eng. J.* **2021**, *60*, 4797–4808. [[CrossRef](#)]
31. Lemarre, P.; Pujo-Menjouet, L.; Sindi, S.S. A Unifying Model for the Propagation of Prion Proteins in Yeast Brings Insight into the [PSI⁺] Prion. *PLoS Comput. Biol.* **2020**, *16*, e1007647.
32. Cong, N.D.; Tuan, H.T. Existence, Uniqueness and Exponential Boundedness of Global Solutions to Delay Fractional Differential Equations. *Mediterr. J. Math.* **2017**, *14*, 193. [[CrossRef](#)]
33. Katugampola, U.N. Existence and Uniqueness Results for a Class of Generalized Fractional Differential Equations. *arXiv* **2016**, arXiv:1411.5229.
34. Erturk, V.S.; Kumar, P. Solution of a COVID-19 Model via New Generalized Caputo-Type Fractional Derivatives. *Chaos Solitons Fractals* **2020**, *139*, 110280. [[CrossRef](#)]

Disclaimer/Publisher's Note: The statements, opinions and data contained in all publications are solely those of the individual author(s) and contributor(s) and not of MDPI and/or the editor(s). MDPI and/or the editor(s) disclaim responsibility for any injury to people or property resulting from any ideas, methods, instructions or products referred to in the content.